Apparent efficiency of serially coupled columns in isocratic and gradient elution modes

AUTHORS: Szabolcs FEKETE[1]*, Santiago CODESIDO[1], Serge RUDAZ[1], Davy GUILLARME[1], Krisztián HORVÁTH[2]

[1] School of Pharmaceutical Sciences, University of Geneva, University of Lausanne, CMU - Rue Michel Servet, 1, 1211 Geneva 4 – Switzerland

[2] Department of Analytical Chemistry, University of Pannonia, Egyetem u. 10, 8200 Veszprém, Hungary

CORRESPONDENCE: Szabolcs FEKETE

Phone: +41 22 379 63 34

E-mail: szabolcs.fekete@unige.ch

Apparent efficiency of serially coupled columns in isocratic and gradient elution modes

Abstract

The goal of this work was to understand the variation of apparent efficiency when serially coupling columns with identical stationary phase chemistries, but with differences in their kinetic performance. For this purpose, a mathematical treatment was developed both for isocratic and gradient modes to assess the change in plate numbers and peak widths when coupling arbitrary several columns. To validate the theory, experiments were also carried out using various mixtures of compounds, on columns packed with different particle sizes, to mimic highly efficient (new, not used) and poorly efficient columns (used one with many injections). Excellent agreement was found between measured and calculated peak widths. The average error in prediction was about 5 % (which may be explained by the additional volume of the coupling tubes).

In isocratic mode, the plate numbers are not additive when the coupled columns possess different efficiencies, and a limiting plate count value can be calculated depending on the efficiency and length of the individual columns. Theoretical efficiency limit can also be determined assuming one column in the row with infinite efficiency.

In gradient elution mode, the columns' order has a role (non-symmetrical system). When the last column has high enough efficiency, the gradient band compression effect may outperform the competing band broadening caused by dispersive and diffusive processes (peak sharpening). Therefore, in gradient mode, the columns should generally be sequentially placed according to their increasing efficiency.

Keywords:

Column coupling, apparent efficiency, plate number, peak capacity, column length

1. Introduction

The idea of coupling columns to analyze complex samples appeared quite early in chromatography [1,2,3,4,5,6]. The purpose of column coupling can be either to improve kinetic performance by increasing the column length or adjust selectivity by combining different stationary phase chemistries. This latter idea lead to the development of multidimensional chromatographic separations.

There are two ways to combine two or more columns in mono-dimensional separations, namely parallel and serial arrangements [7]. Serial columns generally outperform parallel setups, as the resolution power is appreciably extended in this configuration. The effect of changes in column length is different in the serial and parallel approaches. The serially coupled columns approach has an intrinsic advantage: there is an additional separation factor (the column length), which however has no consequence in the experimental effort. In practice, each serial combination of short columns of different chemical nature and length operates as a new column, with its own selectivity. This increases enormously the wealth of columns available in a laboratory, from which the best one can be selected for a given application [7].

In most cases, the aim of column coupling remains to increase the chromatographic performance. The kinetic plot method (KPM) is often used as a design tool to find out the optimal column length to achieve a given number of theoretical plates [8,9]. The KPM can be used to predict the analysis time and efficiency which vary over a wide range of different column lengths, from very short to very long columns. Although the length independence is implicitly contained in the definition of the plate height concept, there are a number of cases wherein deviations from this behavior can be expected (axial temperature gradient due to viscous heating, extra-column band broadening effects which have relatively higher impact on small columns, side-wall effects that persist along the column length, pressure-related effects, etc.) [10,11,12,13]. The possibility to predict the performance of coupled columns systems has been extensively studied in the past. Coupling of up to six columns (900 mm = 6 x 150 mm) showed that the KPM prediction was in good agreement with the obtained

performance on the coupled column system [14]. In another study [15], it has been demonstrated that up to 8 columns (packed with 5 μm particles) could be coupled in series and operated at a constant flow rate without any significant loss of efficiency, again implying that the observed plate heights were independent on the column length.

The best combination of coupled columns in isocratic mode having different lengths and particle sizes was determined in a previous study from Cabooter *et al.* based on the Knox-Saleem speed limit [16]. Considering an ultrahigh-performance liquid chromatography (UHPLC) system operating at a pressure of 1200 bar, the best possible serial connection system can approach the 75–85 % of its Knox-Saleem limit whereas a three-column parallel system can only get about 50–60 % of the speed limit, while needing 50–100 % more total column length. In absolute terms, the serially-connected system with individually optimized segment lengths should be able to cover a range of 5000–75,000 theoretical plates in an average analysis time of 14.3 min when using a 1200 bar instrument [16].

When working in gradient mode, the overall peak capacity can be predicted in a very similar way on the basis of peak capacity measured on one single column, and assuming no differences in the performance of columns that will be coupled in series. Peak capacity prediction has indeed shown very good accuracy when coupling four columns of 150 mm in series [17]. Despite neglecting the possible variations in performance of the individual columns (different batches, history of the column), the kinetic performance limit approach works well in practice, as long as chromatographers couple the same type of columns (same stationary phase and dimension) in series.

Therefore, in isocratic mode the plate numbers are expected to be additive, while in gradient mode, the peak capacity is proportional with the square root of the column length [18].

Serial column coupling can be useful for various types of applications and is particularly used in RPLC mode [19]. By using a 450 mm long column (3 x 150 mm), the peak capacity of an antibody peptide mapping analysis was increased up to n_c = 704 [20]. The same concept has also been used for intact and sub-units antibody analysis [20]. Another study showed the possibilities to achieve high plate count and peak capacity at various combinations of column

lengths and temperatures [21]. Column coupling has also been applied in ion-exchange (IEX) chromatography to improve the separation of intact antibody charge-variants [22]. In supercritical fluid chromatography (SFC), 4 columns (4 x 100 mm) were successfully coupled to increase the separation of 24 pharmaceutical compounds [23]. Column coupling can also be applied for chiral separations [24]. As an example, an in-line coupling of achiral and chiral columns was shown to be a good alternative to multidimensional chiral chromatography [24]. Coupling columns of different pore sizes in series is also commonly used in size exclusion chromatography (SEC) to tune the selectivity of polymer separations [25].

Other purposes of column coupling can be post-column derivatization, on-line clean-up or the protection of the analytical column by using guard (pre-) columns [26,27].

The purpose of this study was to estimate and measure the apparent efficiency of columns made of identical stationary phase chemistry but possessing differences in their kinetic performance. It may happen that the individual columns do not have identical efficiency (different batch, different lifetime and antecedents, or different packing quality which is well-known to be dependent on column length and diameter [28]). Different particle sizes were used to mimic columns of different batches or columns providing different efficiencies when coupling them in series. In isocratic mode, the plate numbers do not always seem additive and kinetic performance has a limiting value, depending on the efficiency and length of the individual columns. Furthermore, in gradient elution mode, the system is indifferent to the column order. Theory has been developed to show the evolution of plate numbers for coupling arbitrary several columns in isocratic mode and to predict peak widths for two columns system in gradient mode. Experimental measurements have been performed to validate the theory.

2. Theory

2.1 Peak widths in isocratic elution

The band dispersion in serially connected columns can be calculated by solving the following ordinary differential equation:

$$\frac{d\sigma_z^2}{dz} = H(z) \quad (1)$$

where σ_z^2 is the spatial variance of bands of compounds inside the column, z the spatial variable, and $H(\mathrm{z})$ the height equivalent to a theoretical plate, HETP.

$$H(z) = H_i \quad if \quad \sum_{j=0}^{i-1} L_j \leq z < \sum_{j=1}^{i} L_j \quad (2)$$

where H_i and L_i are the HETP and length of the i^{th} column, respectively. Note that L_0 is equal to zero.

The solution of Eq. (1) in case of n sequentially connected columns with the initial condition $\sigma_z^2(0) = 0$ is:

$$\sigma_z^2 = \sum_{i=1}^{n} L_i H_i = \sum_{i=1}^{n} \frac{L_i^2}{N_i} \quad (3)$$

Assuming that retention factors (k) of solutes are the same in all the columns (identical stationary phase chemistry), the retention time of a compound can be expressed as:

$$t_R = \sum_{i=1}^{n} t_{R,i} = (1+k) \sum_{i=1}^{n} t_{0,i} = (1+k) \sum_{i=1}^{n} \frac{L_i}{u_{0,i}} \quad (4)$$

where $t_{0,i}$ is the hold-up time, and $u_{0,i}$ is the average linear velocity of the eluent in the i^{th} column.

By matching the spatial (σ_z) and time (σ) variances through the definition of efficiency and replacing t_R by Eq. (4), the following is obtained for a chromatographic peak eluted from n sequentially connected columns is:

$$\sigma^2 = \sigma_z^2 \frac{(1+k)^2}{u_{0,n}^2} \quad (5)$$

The fraction on the right hand side of Eq. (5) can be expressed from Eq. (4) as:

$$\frac{1+k}{u_{0,n}} = \frac{t_R}{L_n} \frac{V_{0,n}}{V_0} \quad (6)$$

where L_n and $V_{0,n}$ are the length and dead volume of the last segment, V_0 is the total dead volume of the n sequentially connected columns. Explicitly, $V_{0,i} = L_i \frac{d_i^2 \pi}{4} \varepsilon_i$ with d_i and ε_i are the internal diameter and total porosity of column i.

149 Eq. (6) can be combined with Eq. (5) and the peak width can be calculated as:

150 $$w = 4\sigma = 4\sqrt{\sum_{i=1}^{n} \frac{L_i^2}{N_i} \frac{t_R}{L_n} \frac{V_{0,n}}{V_0}} = 4\alpha t_R \quad (7)$$

151 where,

152 $$\alpha = \frac{1}{L_n}\sqrt{\sum_{i=1}^{n} \frac{L_i^2}{N_i} \frac{V_{0,n}}{V_0}} \quad (8)$$

153 The total plate number of the sequentially connected columns is the sum of the number of
154 theoretical plates of the n columns. The apparent plate number, however, can be calculated
155 as:

156 $$N_{app} = \frac{t_R^2}{\sigma^2} = \frac{1}{\alpha^2} \quad (9)$$

157 Eqs. (8) and (9) can be generalized after the following considerations:

158 $$\lambda_i = \frac{L_i}{L_n},\ \nu_i = \frac{N_i}{N_n},\ \omega_i = \frac{V_{0,i}}{V_{0,n}} \quad (10)$$

159 Accordingly,

160 $$\alpha = \frac{1}{\sqrt{N_n}}\sqrt{1 + \sum_{i=1}^{n-1} \frac{\lambda_i^2}{\nu_i} \frac{1}{1+\sum_{i=1}^{n-1}\omega_i}} \quad (11)$$

161 and,

162 $$N_{app} = N_n \frac{\left(1+\sum_{i=1}^{n-1}\omega_i\right)^2}{1+\sum_{i=1}^{n-1}\frac{\lambda_i^2}{\nu_i}} \quad (12)$$

163 The ratio of N_{app} and the total plate number is:

164 $$\frac{N_{app}}{\sum_{i=1}^{n} N_i} = \frac{\left(1+\sum_{i=1}^{n-1}\omega_i\right)^2}{\left(1+\sum_{i=1}^{n-1}\nu_i\right)\left(1+\sum_{i=1}^{n-1}\frac{\lambda_i^2}{\nu_i}\right)} \quad (13)$$

165 For a two-column system Eqs. (11), (12) and (13) become:

166 $$\alpha = \frac{1}{\sqrt{N_2}}\sqrt{1 + \frac{\lambda_1^2}{\nu_1} \frac{1}{1+\omega_1}} \quad (14)$$

167 $$N_{app} = N_2 \frac{(1+\omega_1)^2}{1+\frac{\lambda_1^2}{\nu_1}} \quad (15)$$

168 $$\frac{N_{app}}{N_1+N_2} = \frac{(1+\omega_1)^2}{(1+\nu_1)\left(1+\frac{\lambda_1^2}{\nu_1}\right)} \quad (16)$$

There are also several specific situations for two-columns:

If the plate numbers of the two columns are equal:

$$N_{app} = \frac{N}{1+\frac{L_1^2}{L_2^2}}\left(1+\frac{V_{0,1}}{V_{0,2}}\right)^2 \quad (17)$$

If the column diameters are equal:

$$N_{app} = \frac{N_1 N_2}{N_1+\frac{L_1^2}{L_2^2}N_2}\left(1+\frac{L_1}{L_2}\right)^2 \quad (18)$$

If the column diameters and lengths are equal:

$$N_{app} = 4\frac{N_1 N_2}{N_1+N_2} \quad (19)$$

If the plate numbers and diameters of the two columns are equal:

$$N_{app} = N\frac{(L_1+L_2)^2}{L_1^2+L_2^2} \quad (20)$$

If the efficiency of one of the two columns is infinite ($N_2 = \infty$)

$$N_{app} = N_1\frac{L_2^2}{L_1^2}\left(1+\frac{V_{0,1}}{V_{0,2}}\right)^2 \quad (21)$$

If the efficiency of one of the two columns is infinite ($N_2 = \infty$)) and the column dimensions are identical:

$$N_{app} = 4N_1 \quad (22)$$

Peak capacity, n, can be obtained as the solution of the following ordinary differential equation with the initial condition of $n(t_1) = 1$:

$$\frac{dn}{dt} = \frac{1}{w} \quad (23)$$

where w is peak width as a function of time, t.

The peak capacity of a series of columns connected together in isocratic mode can then be calculated as the solution of Eq. (23):

$$n = 1+\frac{1}{4\alpha}ln\frac{t_n}{t_1} = 1+\frac{\sqrt{N_{app}}}{4}ln\frac{t_n}{t_1} \quad (24)$$

For a two-columns system, the following equation can be written:

$$n = 1 + \frac{1}{4}\sqrt{\frac{N_1 N_2}{N_1 + \frac{L_1^2}{L_2^2} N_2}}\left(1 + \frac{V_{0,1}}{V_{0,2}}\right) ln\frac{t_n}{t_1} \quad (25)$$

If the column dimensions are identical and one of the columns has an infinite efficiency (N_2 = ∞):

$$n = 1 + \frac{\sqrt{N}}{2} ln\frac{t_n}{t_1} \quad (26)$$

2.2 Peak widths in gradient elution

In gradient chromatography, the arrival time of a peak to a position *z* along the column is no longer just proportional to time, but has to be retrieved from solving a differential equation, given by:

$$\frac{dt}{dz} = \frac{1}{u} \ , \qquad t(0) = 0 \quad (27)$$

where the velocity *u* is given by the instantaneous linear velocity of the solute, related to that of the mobile phase (u_0) through the solute retention (*k*):

$$u = \frac{u_0}{1+k} \quad (28)$$

Notice that the condition $t(0) = 0$ implies a negligible dwell volume. This is always the case for initially highly retained compounds, that are stopped at the head of the column until the gradient releases them. According to the linear solvent strength (LSS) theory, the retention factor can be written as a function of the mobile phase composition [29]:

$$k = k_w e^{-S\phi} \quad (29)$$

where *S* is the slope of the LSS model (log k *vs.* % organic modifier) and k_w is the extrapolated value of *k* for a compound eluted with pure A eluent (i.e., Φ=0). When running a linear gradient over a time t_G the mobile phase composition at the inlet of the column is given by:

$$\phi = \phi_0 + \frac{t}{t_G}\Delta\phi \quad (30)$$

The retention at a time *t* and position *z*, taking into account the time $z\, t_0/L$ it takes for the mobile phase to reach that point, will be (again neglecting the dwell volume):

$$k = k_0 exp\left\{-b\left(\frac{t}{t_0} - \frac{z}{L}\right)\right\} \quad (31)$$

where $k_0 = k_w e^{-S\phi_0}$ is the initial retention, L the length of the column, $t_0 = L/u_0$ the hold-up time, and:

$$b = S\Delta\phi\,\frac{t_0}{t_G} \quad (32)$$

Is the intrinsic gradient steepness.

The solution of (27) is the well-known chromatography formula:

$$t(z) = t_0\left[\frac{z}{L} + \frac{1}{b}ln\left(1 + k_0 b\,\frac{z}{L}\right)\right] \quad (33)$$

The time to travel to $z = L$ is the retention time, expressed as:

$$t_R = t(L) = t_0\left[1 + \frac{1}{b}ln(1 + k_0 b)\right] \quad (34)$$

Peak width is mostly affected by diffusion and dispersion processes and by the gradient band compression effect. The peak is compressed because of the changes to its trajectory while crossing the gradient within the column. During gradient elution, the rear part of the peak moves faster than its front part, because the mobile phase strength increases along the column. The steeper the gradient, the higher the band compression effect is. To model the band compression effect, it is useful to consider a peak between a point z and $\tilde{z} = z + \sigma_z$. Then the next formula can be written:

$$\frac{d\sigma_z}{dt} = \frac{d\tilde{z}}{dt} - \frac{dz}{dt} = u(\tilde{z}, t) - u(z, t) = u(z + \sigma_z, t) - u(z, t) \quad (35)$$

When w is small compared to the total length over which the motion of the peak is integrated, the right-hand side of *eq* (35) can be expanded at first order in *w* to obtain:

$$\frac{d\sigma_z}{dt} = \partial_z u(z, t) \cdot \sigma_z \quad (36)$$

Our goal is to have z as an independent variable, so with the chain rule, the following equation can be obtained:

$$\frac{d\sigma_z}{dz} = \frac{d\sigma_z}{dt}\frac{dt}{dz} = \frac{\partial_z u}{u}\sigma_z = \partial_z \ln u \cdot \sigma_z \quad (37)$$

The speed gradient at a given position is obtained by plugging in the solution the equation (33):

$$\partial_z \log u\left(z, t(z)\right) = \frac{-1}{L}\frac{p}{1+\frac{pz}{L}} \tag{38}$$

where,

$$p = b\frac{k_0}{1+k_0} \tag{39}$$

is a measure of the gradient steepness. It takes into account that initially unretained substances ($k_0 = 0$) will not be compressed at all.

The band broadening effects can be dependent on the column HETP measured in isocratic mode, which we call here H_0,

$$\frac{d\sigma_z^2}{dz} = H_0 \tag{40}$$

Equation (40) can be joined with (37) to give:

$$\frac{d\sigma_z^2}{dz} = H_0 + 2\partial_z \log u \cdot \sigma_z^2 \tag{41}$$

If the width $\sigma_{z,0}^2$ at a given point along the column z_0 (this will be necessary for the coupling) is known:

$$\sigma_z^2(z_0) = \sigma_{z,0}^2 \tag{42}$$

the solution is:

$$\sigma_z^2(z) = \frac{\sigma_{z,0}^2\left(1+\frac{pz_0}{L}\right)^2 + H_0(z-z_0)\left(1+\frac{p(z+z_0)}{L}+\frac{1}{3}\frac{p^2\left(z^2+zz_0+z_0^2\right)}{L^2}\right)}{\left(1+\frac{pz}{L}\right)^2} \tag{42}$$

By neglecting the initial peak width caused by the injection process, $\sigma_{z,0}^2 = 0$ when $z = 0$, we obtain the known formula at elution ($z = L$):

$$\sigma_z^2(L) = H_0 L\frac{1+p+\frac{1}{3}p^2}{(1+p)^2} \tag{43}$$

We now assume a two-column system possessing different HETP values, H_1 for length L_1, and H_2 for length L_2. If the same gradient steepness and linear velocity are considered on the two columns, then the migration can still be described by equation (33), with $L = L_1 + L_2$. In the first column, the width evolves from the injection width $\sigma_{z,i}$ at $z = 0$. By setting $H_0 = H_1$, $\sigma_{z,0} = \sigma_{z,i}$ and $z_0 = 0$ in equation (42), the following equation can be obtained:

$$\sigma_{z,1}^2(z) = \frac{\sigma_{z,i}^2 + H_1 z\left(1+\frac{pz}{L}+\frac{1}{3}\left(\frac{pz}{L}\right)^2\right)}{\left(1+\frac{pz}{L}\right)^2} \quad (44)$$

When it reaches $z = L_1$, it starts migrating under H_2. The coupling condition is:

$$\sigma_{z,2}^2(L_1) = \sigma_{z,1}^2(L_1) \quad (45)$$

This means that $\sigma_{z,2}$ follows equation (42), with $H_0 = H_2$, $z_0 = L_1$ and $\sigma_{z,0}^2 = \sigma_{z,1}^2$ (L_1), thus defining:

$$\theta = \frac{(H_1 - H_2)}{H_2} = \frac{H_1}{H_2} - 1 \quad (46)$$

the solution becomes:

$$\sigma_{z,2}^2(z) = \frac{\sigma_{z,i}^2 + H_2 z\left[\left(1+\frac{L_1}{z}\theta\right)+\frac{pz}{L}\left(1+\left(\frac{L_1}{z}\right)^2\theta\right)+\frac{1}{3}\left(\frac{pz}{L}\right)^2\left(1+\left(\frac{L_1}{z}\right)^3\theta\right)\right]}{\left(1+\frac{pz}{L}\right)^2} \quad (47)$$

or over the whole coupled system:

$$\sigma_z(z) = \begin{cases} \sigma_{z,1}(z) & if \quad 0 \leqslant z \leqslant L_1 \\ \sigma_{z,2}(z) & if \quad L_1 \leqslant z \leqslant L \end{cases} \quad (48)$$

The result is very similar to (44), with a correction factor proportional to θ. At elution, $z = L = L_1 + L_2$:

$$\sigma_{z,e}^2 = \sigma_{z,2}^2(L) = \frac{\sigma_{z,i}^2 + H_2 L\left[\left(1+\frac{L_1}{L}\theta\right)+p\left(1+\left(\frac{L_1}{L}\right)^2\theta\right)+\frac{1}{3}p^2\left(1+\left(\frac{L_1}{L}\right)^3\theta\right)\right]}{(1+p)^2} \quad (49)$$

Please note that the dependence in H_1 only comes through θ. In particular, if L_1 is smaller than L, then the efficiency is basically dominated by the second column.

3. Experimental

3.1 Chemicals and columns

Acetonitrile, methanol and ethanol (gradient grade) were purchased from Sigma-Aldrich (Buchs, Switzerland). Water was obtained with a Milli-Q Purification System from Millipore (Bedford, MA, USA).

Uracil, methylparaben, ethylparaben, propylparaben, butylparaben, cannabidivarine (CBDV), cannabigerolic acid (CBGA), tetrahydrocannabivarin (THCV), cannabichromene (CBC), delta9-tetrahydrocannabinolic acid (THCA-A) and human serum albumin (HSA), were

purchased from Sigma–Aldrich. Cannabidiolic acid (CBDA), cannabigerol (CBG), cannabidiol (CBD), cannabinol (CBN), (-)-delta9-THC (d9-THC) and (-)-delta8-THC (d8-THC) were purchased from Lipomed AG (Arlesheim, Switzerland).

Ammonium hydroxide solution, formic acid (FA), trifluoroacetic acid (TFA), dithiothreitol (DTT) and trypsin were obtained from Sigma-Aldrich.

X-Bridge C18 (5 μm, 150 x 4.6 mm) (A), X-Bridge C18 (3.5 μm, 100 x 4.6 mm) (B) and X-Bridge C18 (2.5 μm, 75 x 4.6 mm) (C) columns were purchased from Waters (Milford, MA, USA). Jupiter C18 (5 μm 300 Å, 150 x 2.0 mm) (D) and Jupiter C18 (3 μm 300 Å, 150 x 2.0 mm) (E) columns were purchased from Phenomenex (Torrance, CA, USA).

3.2 Equipment and software

The measurements were performed using a Waters Acquity UPLC™ I-Class system equipped with a binary solvent delivery pump, an autosampler and UV detector and/or fluorescence detector (FL). The system includes a flow through needle (FTN) injection system equipped with 15 μL needle, a 0.5 μL UV flow-cell and a 2 μL FL flowcell. The connection tube between the injector and column inlet was 0.003" I.D. and 200 mm long (active preheating included), and the capillary located between the column and detector was 0.004" I.D. and 200 mm long. The overall extra-column volume (V_{ext}) was about 8.5 μL and 11 μL as measured from the injection seat of the auto-sampler to the detector cell (UV and FL, respectively). The average extra-column peak variance of our system was found to be around σ_{EC}^2 ~0.5 − 3 μL^2 (depending on the flow rate, injected volume, mobile phase composition and solute). Data acquisition and instrument control were performed by Empower Pro 3 Software (Waters).

3.3 Chromatographic conditions and sample preparation

3.3.1. Apparent plate numbers: Isocratic measurements of parabens and uracil

A mix solution containing uracil, methylparaben, ethylparaben, propylparaben and butylparaben was prepared in 80 : 20 v/v water : acetonitrile at 50 μg/mL.

For isocratic chromatographic measurements, the mobile phase was composed of 55 : 45 v/v water : acetonitrile. Experiments were performed at a flow rate of 1 mL/min at ambient temperature. Detection was carried out at 254 nm (40 Hz), the injection volume was 5 μL. The plate numbers were measured on three single columns, namely the 5 μm, 150 x 4.6 mm (A), 3.5 μm, 100 x 4.6 mm (B) and 2.5 μm, 75 x 4.6 mm (C) columns, then the columns were coupled in series using 5 cm long (0.175 mm ID) stainless steel tubing and the apparent plate numbers were measured. The following combinations were tested: (1) columns A + B, (2) columns A + C, (3) columns B + C and (4) columns A + B + C.

3.3.2. Apparent peak widths: gradient measurements of small molecules (mix of cannabinoids)

A mix solution containing eleven cannabinoids (i.e. CBDV, CBGA, THCV, CBC, THCA-A, CBDA, CBG, CBD, CBN, d9-THC and d8-THC) was prepared from individual stock solutions diluted in solvent having the same composition as the initial mobile phase (55 : 45 v/v 10 mM ammonium-acetate : acetonitrile) at 90 μg/mL. The individual stock solutions were prepared in either methanol, acetonitrile or ethanol depending on their solubility. Mobile phase “A” was 10 mM ammonium-acetate (pH = 5.8), mobile phase “B” was acetonitrile. Linear gradients were run from 45 %B to 100 %B at 1 mL/min flow rate and ambient temperature. The gradient time (t_G) over column length (L) ratio was kept constant (t_G/L=1 min/cm) when running gradients on different column lengths (corresponds to e.g. t_G = 10 min on 10 cm long column). Detection was carried out at 220 and 254 nm (40 Hz), the injection volume was 10 μL. The peak widths (peak capacity) were measured on three single columns, namely on the 5 μm, 150 x 4.6 mm (A), 3.5 μm, 100 x 4.6 mm (B) and 2.5 μm, 75 x 4.6 mm (C) columns, and then these columns were coupled in series using 5 cm long (0.175 mm ID) stainless steel tubing, and the apparent peak widths (peak capacity) were measured. The following

combinations were used: (1) columns A + B, (2) columns A + C, (3) columns B + C and (4) columns A + B + C.

3.3.3. Apparent peak widths: gradient measurements of peptides (HSA tryptic digest)

Tryptic digestion of human serum albumin (HSA) was carried out as described in a recent protocol [30]. Mobile phase "A" was 0.1 % TFA in water, mobile phase "B" was 0.1 % TFA in acetonitrile. Linear gradients were run from 10 to 70 %B at a flow rate of 0.3 mL/min and 50 ˚C. The gradient time (t_G) over column length (L) ratio was kept constant (t_G/L=2 min/cm) when running gradients on different column lengths (corresponds to e.g. t_G = 30 min on 15 cm long column). Fluorescence detection was carried out at 280 nm as excitation and 350 nm as emission wavelengths, the injection volume was 5 µL. The peak widths (peak capacity) were measured on two widepore columns of 5 µm, 150 x 2.0 mm (D) and 3 µm, 150 x 2.0 mm (E) columns, then these two columns were coupled in series using 5 cm long (0.175 mm ID) stainless steel tubing, and the apparent peak widths (peak capacity) were measured. The following combinations were used: (1) columns D + E and (2) columns E + D.

4. Results and Discussion

4.1. Apparent plate number in isocratic mode for serially coupled columns

As it is possible to couple together two columns possessing different lengths and efficiencies, an informative representation of the apparent plate number (N_{app}) can be obtained when plotting the ratio of N_{app}/N_{sum} (where N_{sum} is the sum of the individual plate counts) as a function of N_1/N_2 (corresponding to the efficiency of the first and second columns, respectively). In this type of representation, various ratios of column lengths (L_1/L_2) can be tested. Figure 1 shows some plots for L_1/L_2 = 0.75, 1, 1.5 and 2 (calculations are based on eq 18). As suggested by the theory, all the curves show a maxima (N_{app}/N_{sum} = 1), indicating that the highest reachable efficiency with two serially coupled columns is equal to the sum of the individual plate numbers. However, it only occurs at a given ratio of column lengths. When coupling two columns of identical lengths (L_1/L_2 = 1) in series, then this maximum

occurs when the columns possess identical plate numbers ($N_1/N_2 = 1$). When the first column is twice longer than the second one ($L_1/L_2 = 2$), then the maximum plate number is attained when the first column performs twice as high plate numbers than the second one ($N_1/N_2 = 2$). Similarly, when $L_1/L_2 = 1.5$ and 0.75, the maximum performance is expected for $N_1/N_2 = 1.5$ and 0.75, respectively. Accordingly, to obtain the maximum efficiency from equal coupled columns configuration, it is required that their plate heights should be the same. In this case, the apparent plate count is the sum of the individual plate counts. In any other case, N_{app}/N_{sum} will be smaller than 1. An important feature of the system is its symmetric property, meaning that the system (or N) is indifferent to the order. One can choose the more efficient column either in the first or the second position, without affecting the global efficiency.

Table 1 shows the measured and calculated plate numbers on single columns (A, B and C) and serially coupled configurations (including two and three columns) for four model compounds (parabens). As shown, the measured and predicted plate numbers are in very good agreement, with a variation between measured and predicted efficiency comprised between -7 and +5 %. Figure 1 also includes the experimentally measured values which fit quite well with the theoretical curves. As an example, Figure 2 shows some representative chromatograms of the four parabens separated on three different columns with different lengths and efficiency as well as with the three columns serially coupled.

Another interesting aspect is to track the efficiency increase of two serially coupled columns compared to just one of the columns used for this coupling. Figure 3 illustrates N_{app}/N_1 as a function of N_1/N_2 for three cases, namely for $L_1/L_2 = 0.2$, 1 and 2 with identical column diameters. When $L_1/L_2 = 2$ (the first column is twice as long as the second one), the intercept of the curve corresponds to $N_{app}/N_1 = 2.25$. This means that the maximum efficiency is 2.25 times higher *vs.* that of the first column. It occurs when the second column has infinite efficiency (intercept at $N_1/N_2=0$). In this case, the second column only increases retention times without any effect on band broadening. As illustrated in Figure 3, it is not possible to attain higher plate numbers with this setup. On the other hand, if the efficiency of the second column is five times lower than that of the first column, then the apparent plate number of

serially coupled columns will be the same as of the first column. When N_1/N_2 is above 5, the overall efficiency of the coupled system is lower than the efficiency of the first column. This means that it is possible to combine two HPLC columns that finally generate lower resolution than that offered by the most efficient column alone. This counter instinctive consequence is analogous to the band broadening effect due to the extra column contributions. Similarly, when $L_1/L_2 = 1$, the maximum achievable efficiency is four times higher than that of the first column, while if the efficiency of the second column is at least three times lower than the first column, then no increase in efficiency is obtained when coupling these two columns. Finally, when the first column is very short compared to the second column ($L_1/L_2 = 0.2$) and the second column has very high efficiency (infinite) then $N_{app}/N_1 = 36$ can be attained when coupling the columns.

In general, when efficiency of the second column is infinite, the apparent plate number of the two-column system becomes:

$$N_{app} = N_1 \left(\frac{1+\lambda}{\lambda}\right)^2 \quad (50)$$

The condition when additional gain of efficiency can be obtained by coupling two columns is:

$$\nu < 1 + 2\lambda \quad (51)$$

or similarly,

$$\xi > \frac{\lambda}{1+2\lambda} \quad (52)$$

where $\nu = N_1/N_2$, $\lambda = L_1/L_2$, and $\xi = H_1/H_2$.

Accordingly, additional gain of efficiency and resolution is possible by coupling two HPLC columns only if the column plate heights do not differ too significantly.

4.2. The evolution of peak width and peak capacity in gradient mode for serially coupled columns

In gradient elution mode, the order of the columns is concerned, and the observed apparent efficiency strongly depends on the order of the columns (non-symmetrical system). An illustration is given in Figure 4. Assuming two columns (with the same internal diameter) with

424 plate heights, H = 10 µm and H = 40 µm, respectively coupled in series. The peak width will
425 evolve in different ways depending on the column order and length of the individual
426 segments (the different plate heights were assumed to mimic columns of different batches or
427 the combination of old and new columns). The continuous lines in Figure 4 show the peak
428 widths for coupled columns possessing different efficiencies as a function of the position of
429 the solute (z) along its travel. The dashed lines correspond to columns having either H = 10
430 µm or H = 40 µm efficiency along its entire length (10 cm) – as reference values.
431 Figure 4A shows the case where two segments of 5 cm are coupled at a moderate gradient
432 steepness (p=1). When placing the more efficient column in the first position and the less
433 efficient one in the second position (continuous red line) – as expected – the peak will
434 broaden drastically after entering the second (less efficient) column as the band broadening
435 caused by dispersion and diffusion processes becomes more important. However, when
436 having the less performing column in the first position and the most efficient column in the
437 second position (continuous blue line), interestingly the peak width will decrease
438 continuously during the travel of the solute along the second column ("peak sharpening"). It
439 suggests that the gradient band compression effect outperforms the dispersive and diffusive
440 effects in the second column as the more efficient column offers much lower H value than the
441 first column. If the second - more efficient - column is very long compared to the first one, the
442 peak width will approach the limiting value theoretically obtained only with the more efficient
443 column - indeed, the dashed line (single column with maximal efficiency) is an asymptote of
444 the solid line (coupled system), that are equal in the large z limit.
445 Figure 4B represents a situation where the column lengths are different. The first one is four
446 times shorter than the second one. When placing the better column in the first position, then
447 a trend similar to that of Figure 4A can be seen. However the coupled system approaches
448 faster its limit (see the dashed and continuous red lines) because at the beginning of the
449 solute's travel along the column, the gradient compression effect is stronger than later during
450 the travel (e.q. 38). When putting the more efficient column as the second one, then no band
451 broadening occurs in the second column, and the peak width remains more or less constant

whilst the solute is traveling through the second column (continuous blue line). It suggests that the gradient band compression effect nearly compensates the band broadening caused by dispersion and diffusion processes. Please note that the differences between the coupled systems – with columns possessing different efficiencies - were larger in this case compared to the situation where the lengths were identical (see the differences at z = 10 cm between the continuous blue and red lines in Figures 4A and 4B).

Finally, figure 4C corresponds to a situation with two columns of 5 cm – similarly to Figure 4A – but for a steeper gradient (p = 10). The trends were similar as the ones observed in Figure 4A, but as expected the gradient focusing effect was more important, and therefore the total peak width was smaller. When placing the better column in the second position (continuous blue line), the speed of peak compression was faster on the second column compared to the case where a flatter gradient was applied.

To verify the theory developed for predicting the peak width in gradient mode, two sets of compounds were analyzed using serially connected columns having different particle sizes and lengths. Figure 5 shows the separations of 11 cannabinoids on three different individual columns and on different combinations of two or three columns, as selected examples. Table 1 contains the experimentally measured and predicted peak widths for the first and last eluting peaks. The peak width prediction for serially coupled columns was based on the peak widths measured on the individual columns. In particular, values for single column efficiencies were retrieved from direct measurements of peak width. These efficiencies were then used as the input for the coupled formula (e.q. 49). The measured and calculated widths were in very good agreement, as the average error in prediction was about 5-6 %.

Another experimental verification was performed by injecting HSA tryptic digest on two individual widepore columns packed with 5 and 3 µm particles and on the combination of these two columns in different orders (Figure 6). Larger molecules (peptides) possess higher S values, therefore it was interesting to check the validity of the model calculations for such molecules. The peak widths of the three most intense (and well separated) peaks was predicted for the coupled systems from the widths on the single columns. Again, very good

agreement was found between experimentally observed and calculated peak widths (Table 3), as the average error in prediction was about 6 %. The results confirm the importance of the columns order as the order “D + E” always gave thinner peaks than “E + D” (both for predicted and measured peak widths).

5. Conclusions

The serially coupled columns approach has an intrinsic advantage as it offers an additional separation factor (the column length). In most cases, the column length is increased by coupling columns packed with the same material (i.e. stationary phase and particle size). In this case, the plate number observed with the coupled column system is the sum of the plate counts observed on the individual column segments. However, it may happen that the individual columns do not have identical efficiency (different batch, different lifetime and antecedents, or different packing quality which is well-known to be dependent on column length and diameter). Therefore, coupling columns with different efficiencies in series raises some questions: (1) What will be the final apparent efficiency?, (2) What is the maximum efficiency that can be reached?, and (3) Does the column order play a significant role?

Theory was developed for both isocratic and gradient modes, to predict the peak widths for coupled column systems. In isocratic mode, the plate numbers are not additive anymore when the columns possess different plate count, and kinetic performance has a limiting value which depends on the efficiency and length of the individual columns.

Furthermore, in gradient elution mode, the order of the columns is not indifferent. Indeed, the observed apparent efficiency significantly depends on the column order (non-symmetrical system). In combinations, when the latter column has higher efficiency, a decrease of the peak width is predicted (“peak sharpening”), when the solute travels this segment. This means that the gradient band compression effect compensates and outperforms the competing band broadening caused by dispersive and diffusive processes. Therefore, the columns should be placed in order of increasing efficiency.

Experimental measurements have been performed in both isocratic and gradient modes to verify the developed theory. Very good agreement was found between measured and calculated peak widths.

To conclude for serially coupled column systems in gradient mode, besides the total length of the coupled column, additional important factors are the order and lengths of the individual segments which must be considered when optimizing a gradient separation.

6. Acknowledgements

The authors wish to thank Jean-Luc Veuthey and Balazs Bobaly from the University of Geneva for fruitful discussions.

Davy Guillarme wishes to thank the Swiss National Science Foundation for support through a fellowship to Szabolcs Fekete (31003A 159494).

Krisztián Horváth acknowledges the financial support of the Hungarian Government and the European Union, with the co-funding of the European Social Fund in the frame of GINOP Programme [Code No: GINOP-2.3.2-15-2016-00016], and of the János Bolyai Research Scholarship of the Hungarian Academy of Sciences.

References

[1] J.L. Glajch, J.C. Gluckman, J.G. Charikofsky, J.M. Minor, J.J. Kirkland, Simultaneous selectivity optimization of mobile and stationary phases in RPLC for isocratic separations of phenylthiohydantoin amino acid derivatives, J. Chromatogr. 318 (1985) 23–39.

[2] P.H. Lukulay, V.L. McGuffin, Solvent modulation in liquid chromatography: extension to serially coupled columns, J. Chromatogr. A 691 (1995) 171–185.

[3] F. Garay, Application of a flow-tunable, serially coupled gas chromatographic capillary column system for the analysis of complex mixtures, Chromatographia 51 (2000) 108–120.

[4] Sz. Nyiredy, Z. Szücs, L. Szepesy, Stationary phase optimized selectivity liquid chromatography: Basic possibilities of serially connected columns using the PRISMA principle, J. Chromatogr.A 1157 (2007) 122–130.

[5] K. Chen, F. Lynen, M. De Beer, L. Hitzel, P. Ferguson, M. Hanna-Brown, P. Sandra, Selectivity optimization in green chromatography by gradient stationary phase optimized selectivity liquid chromatography, J. Chromatogr. A 1217 (2010) 7222-7230.

[6] T. Alvarez-Segura, J.R. Torres-Lapasio, C. Ortiz-Bolsico, M.C. García-Alvarez-Coque, Stationary phase modulation in liquid chromatography through the serial coupling of columns: A review, Anal. Chim. Acta, 923 (2016) 1-23.

[7] T. Alvarez-Segura, C. Ortiz-Bolsico, J.R. Torres-Lapasio, M.C. Garcia-Alvarez-Coque, Serial versus parallel columns using isocratic elution: A comparison of multi-column approaches in mono-dimensional liquid chromatography, J. Chromatogr. A 1390 (2015) 95–102.

[8] G. Desmet, D. Clicq, P. Gzil, Geometry-independent plate height representation methods for the direct comparison of the kinetic performance of LC supports with a different size or morphology, Anal. Chem. 77 (2005) 4058-4070.

[9] D. Cabooter, F. Lestremau, F. Lynen, P. Sandra, G. Desmet, Kinetic plot method as a tool to design coupled column systems producing 100,000 theoretical plates in the shortest possible time, J. Chromatogr. A 1212 (2008) 23–24.

550 [10] U.D. Neue, M. Kele, Performance of idealized column structures under high pressure, J.
551 Chromatogr. A 1149 (2007) 236-244.
552 [11] W.Th. Kok, U.A.Th. Brinkman, R.W. Frei, H.B. Hanekamp, F. Nooitgedacht, H. Poppe,
553 Use of conventinal instrumentation with microbore column in high-performance liquid
554 chromatography, J. Chromatogr. 237 (1982) 357-369.
555 [12] K. Broeckhoven, G. Desmet, Approximate transient and long time limit solutions for the
556 band broadening induced by the thin sidewall-layer in liquid chromatography columns, J.
557 Chromatogr. A 1172 (2007) 25-39.
558 [13] S. Fekete, K. Horvath, D. Guillarme, Influence of pressure and temperature on molar
559 volume and retention properties of peptides in ultra-high pressure liquid chromatography, J.
560 Chromatogr. A 1311 (2013) 65-71.
561 [14] F. Lestremau, A. de Villiers, F. Lynen, A. Cooper, R. Szucs, P. Sandra, High efficiency
562 liquid chromatography on conventional columns and instrumentation by using temperature as
563 a variable: Kinetic plots and experimental verification, J. Chromatogr. A 1138 (2007) 120-
564 131.
565 [15] F. Lestremau, A. Cooper,R. Szucs, F. David, P. Sandra, High-efficiency liquid
566 chromatography on conventional columns and instrumentation by using temperature as a
567 variable: I. Experiments with 25 cm × 4.6 mm I.D., 5 μm ODS columns, J. Chromatogr. A
568 1109 (2006) 191-196.
569 [16] D. Cabooter, G. Desmet, Performance limits and kinetic optimization of parallel and
570 serially connected multi-column systems spanning a wide range of efficiencies for liquid
571 chromatography, J. Chromatogr. A 1219 (2012) 114-127.
572 [17] A. Vaast, J. De Vos, K. Broeckhoven, M. Verstraeten, S. Eeltink, G. Desmet, Maximizing
573 the peak capacity using coupled columns packed with 2.6 μm core–shell particles operated
574 at 1200 bar, J. Chromatogr. A 1256 (2012) 72-79.
575 [18] U.D. Neue, Peak capacity in unidimensional chromatography, J. Chromatogr. A 1184
576 (2008) 107-130.

577 [19] S. Fekete, J.L. Veuthey, D. Guillarme, Comparison of the most recent chromatographic
578 approaches applied for fast and high resolution separations: Theory and practice, J.
579 Chromatogr. A 1408 (2015) 1-14.
580 [20] S. Fekete, M.W. Dong, T. Zhang, D. Guillarme, High resolution reversed phase analysis
581 of recombinant monoclonal antibodies by ultra-high pressure liquid chromatography column
582 coupling, J. Pharm. Biomed. Anal. 83 (2013) 273-278.
583 [21] D. Guillarme, E. Grata, G. Glauser, J.L. Wolfender, J.L. Veuthey, S. Rudaz, Some
584 solutions to obtain very efficient separations in isocratic and gradient modes using small
585 particles size and ultra-high pressure, J. Chromatogr. A 1216 (2009) 3232-3243.
586 [22] S. Fekete, A. Beck, D. Guillarme, Characterization of cation exchanger stationary
587 phases applied for the separations of therapeutic monoclonal antibodies, J. Pharm. Biomed.
588 Anal. 111 (2015) 169-176.
589 [23] A.G.G. Perrenoud, C. Hamman, M. Goel, J.L. Veuthey, D. Guillarme, S. Fekete,
590 Maximizing kinetic performance in supercritical fluid chromatography using state-of-the-art
591 instruments, J. Chromatogr. A 1314 (2013) 288-297.
592 [24] N.C.P. Albuquerque, J.V. Matos, A.R.M. Oliveira, In-line coupling of an achiral-chiral
593 column to investigate the enantioselective in vitro metabolism of the pesticide Fenamiphos
594 by human liver microsomes, J. Chromatogr. A 1467 (2016) 326-334.
595 [25] R. Eksteen, H.G. Barth, B. Kempf, The effect of sec column arrangement of different
596 pore sizes on resolution and molecular weight measurements, LCGC North America, 29
597 (2011) 668–671.
598 [26] A. Jones, S. Pravadali-Cekic, G.R. Dennis, R.A. Shalliker, Post column derivatisation
599 analyses review. Is post-column derivatisation incompatible with modern HPLC columns?,
600 Anal. Chim. Acta, 889 (2015) 58-70.
601 [27] M. Javanbakht, M.M. Moein, B. Akbari-adergani, On-line clean-up and determination of
602 tramadol in human plasma and urine samples using molecularly imprinted monolithic column
603 coupling with HPLC, J. Chromatogr. B, 911 (2012) 49-54.

[28] S. Schweiger, S. Hinterberger, A. Jungbauer, Column-to-column packing variation of disposable pre-packed columns for protein chromatography, J. Chromatogr. A, 1527 (2017) 70-79.

[29] L.R. Snyder, J.W. Dolan, High-performance gradient elution: The practical application of the linear solvent strength model, John Wiley & Sons, Inc. 2007

[30] B. Bobaly, V. D'Atri, A. Goyon, O. Colas, A. Beck, S. Fekete, D. Guillarme, Protocols for the analytical characterization of therapeutic monoclonal antibodies. II – Enzymatic and chemical sample preparation, J. Chromatogr. B 1060 (2017) 325-335.

614 Table 1.

615

column	L (mm)	methylparaben		ethylparaben		propylparaben		butylparaben	
		measured	predicted	measured	predicted	measured	predicted	measured	predicted
A	150	15111	-	14911	-	14763	-	15070	-
B	100	6066	-	6329	-	6512	-	6889	-
C	75	11509	-	12046	-	12478	-	12681	-
A+B	250	19388	19920	19792	20233	19863	20427	20956	21225
A+C	225	24744	25598	24955	25621	25599	25635	25902	26414
B+C	175	14406	14329	15301	14961	15921	15417	16440	16160
A+B+C	325	27857	29128	28757	29704	29256	30088	30690	31174

616

617 Table 2.

618

column	L (mm)	peak 1 $w_{1/2}$ measured (min)	peak 1 $w_{1/2}$ predicted (min)	peak 11 $w_{1/2}$ measured (min)	peak 11 $w_{1/2}$ predicted (min)	Rs crit 9.10	peak capacity
A	150	0.0571	-	0.0715	-	0.69	134
B	100	0.0666	-	0.0771	-	0.55	83
C	75	0.0375	-	0.0399	-	0.57	119
B+A	250	0.0909	0.0993	0.1031	0.1162	0.88	144
C+A	225	0.075	0.0698	0.0838	0.0870	0.99	159
C+B	175	0.0852	0.0861	0.0964	0.0994	0.57	110
A+B+C	325	0.1054	0.0957	0.1098	0.1084	1.00	167

619

620

621 Table 3.

622

column	L (mm)	peak 1		peak 2		peak 3		peak capacity
		$w_{1/2}$ measured (min)	$w_{1/2}$ predicted (min)	$w_{1/2}$ measured (min)	$w_{1/2}$ predicted (min)	$w_{1/2}$ measured (min)	$w_{1/2}$ predicted (min)	
D	150	0.0697	-	0.0703	-	0.0781	-	240
E	150	0.0592	-	0.0559	-	0.0525	-	312
D + E	300	0.0918	0.0857	0.0849	0.0819	0.088	0.0797	388
E + D	300	0.0923	0.0968	0.095	0.0971	0.0966	0.1066	362

623

624

Figure captions

Figure 1. N_{app}/N_{sum} (relative apparent efficiency of the coupled system) as a function of N_1/N_2 (ratio of individual column efficiency) for various column length ratios (L_1/L_2 = 0.75, 1, 1.5 and 2).

Figure 2. Experimentally obtained chromatograms of a mixture of uracil and 4 parabens on columns A, B and C and on serially connected columns A+B+C in isocratic mode. The mobile phase was composed of 55 : 45 v/v water : acetonitrile. Experiments were performed at a flow rate of 1 mL/min at ambient temperature. Detection was carried out at 254 nm (40 Hz), the injection volume was 5 µL. Peaks: uracil (t_0), methylparaben (1), ethylparaben (2), propylparaben (3) and butylparaben (4).

Figure 3. N_{app}/N_1 (apparent efficiency compared to the first column) as a function of N_1/N_2 (ratio of individual column efficiency) for various column length ratios (L_1/L_2 = 0.2, 1, and 2).

Figure 4. The evolution of peak variance (σ_z) along the column (z) for a system composed of two columns coupled in series. Three cases named A to C are reported, corresponding to different segment lengths and gradient steepness, considering H = 10 µm and 40 µm. Please note that time based peak width as a practical measure of band broadening can be obtained at the total length by $= \frac{\sigma_z(L)}{u_0}$.

Figure 5. Experimental chromatograms of cannabinoids mixture on columns A, B and C and on serially connected combinations in gradient mode. Linear gradients were run from 45 to 100 %B at 1 mL/min and ambient temperature. The gradient time (t_G) over column length (L) ratio was kept constant (t_G/L=1 min/cm) when running gradients on different column lengths. Detection was carried out at 254 nm (40 Hz), and injection volume was 10 µL.

Figure 6. Experimental chromatograms of HSA tryptic digest on columns D and E and on serially connected “D+E” and “E+D” combinations in gradient mode. Linear gradients were run from 10 to 70 %B at 0.3 mL/min and 50 ˚C. The gradient time (t_G) over column length (L) ratio was kept constant (t_G/L=2 min/cm) when running gradients on different column lengths. Detection was carried out at 280 nm as fluorescence excitation and 350 nm as fluorescence emission wavelengths, and injection volume was 5 µL.

Table captions

Table 1. Measured and predicted plate numbers for parabens in isocratic mode on three individual columns and on their different combinations. (Predictions are based on eq. 18 for two columns and 12 for three columns.)

Table 2. Measured and predicted peak widths for cannabinoids in gradient elution mode on three individual columns and on their different combinations. The obtained critical resolution and peak capacity are also shown. (Predictions are based on eq. 47-49.)

Table 3. Measured and predicted peak widths for peptides obtained in gradient elution mode on two individual columns and on their combinations. The obtained peak capacity is also indicated. (Predictions are based on eq. 47-49.)

Figure

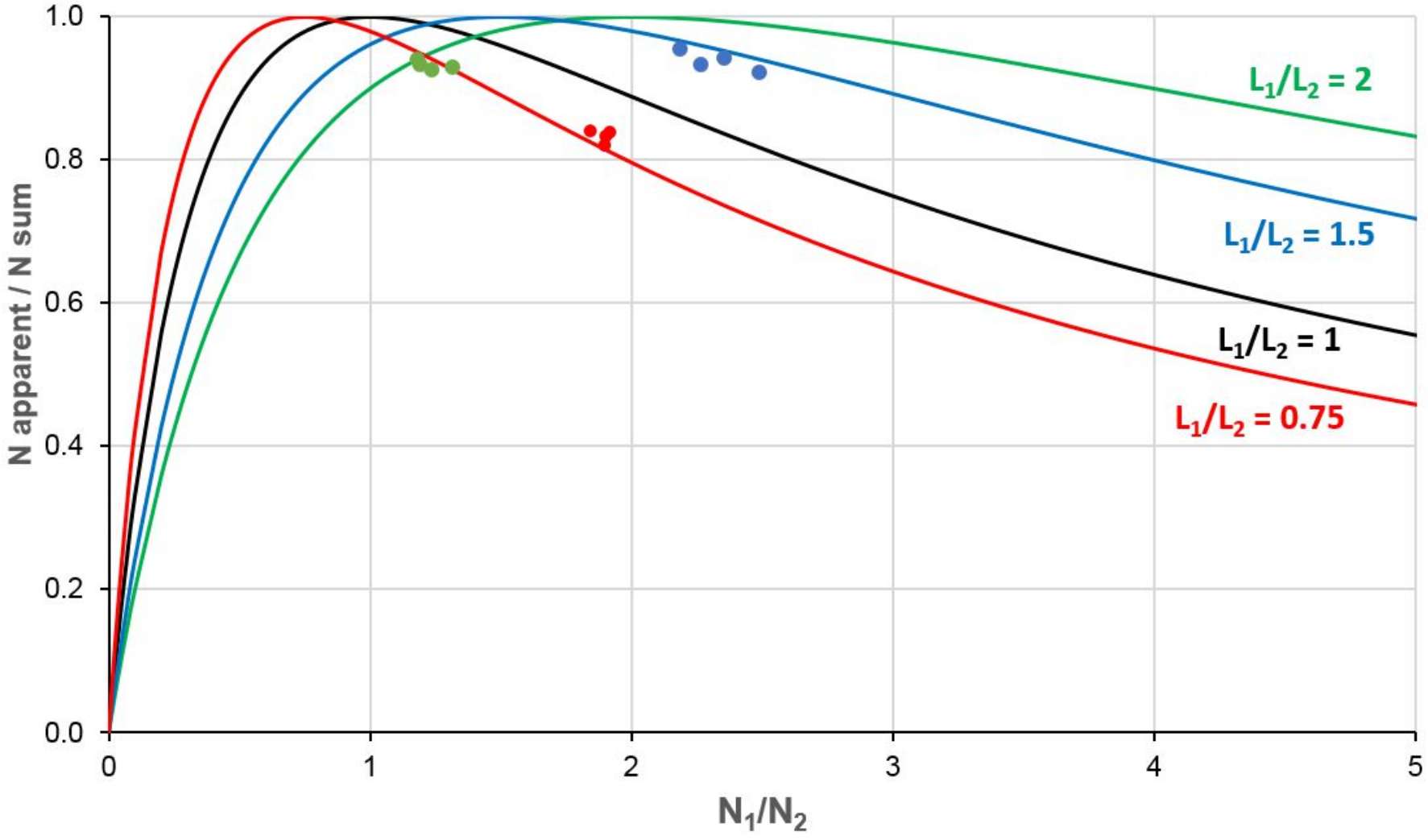

Figure 1

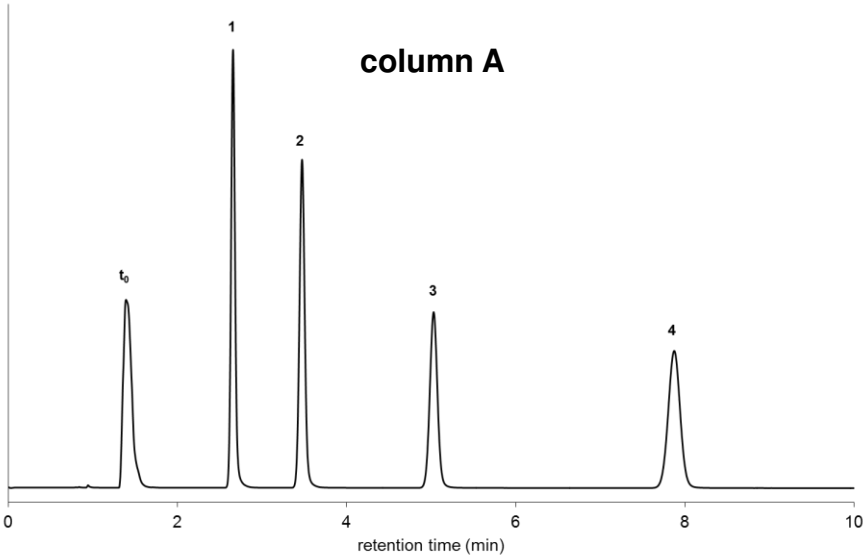
column A
1
2
t0
3
4
0
2
4
6
8
10
retention time (min)

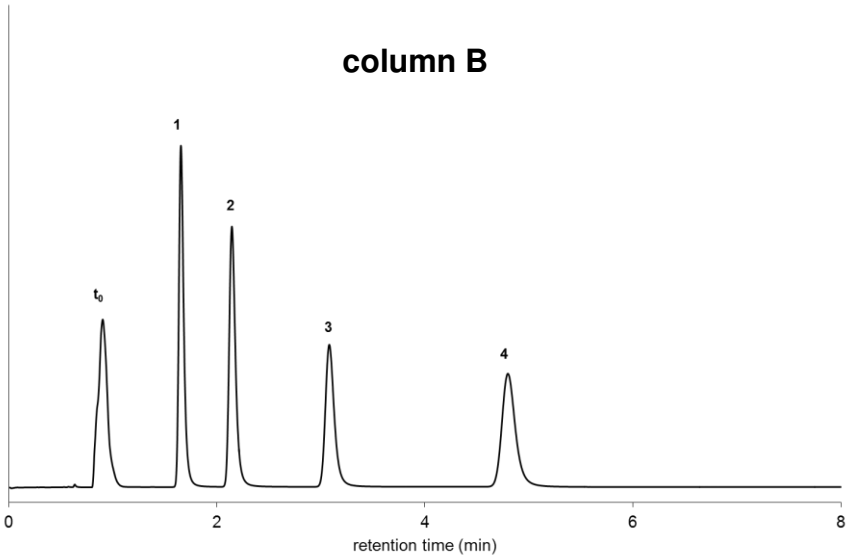
column B
1
2
t0
3
4
0
2
4
6
8
retention time (min)

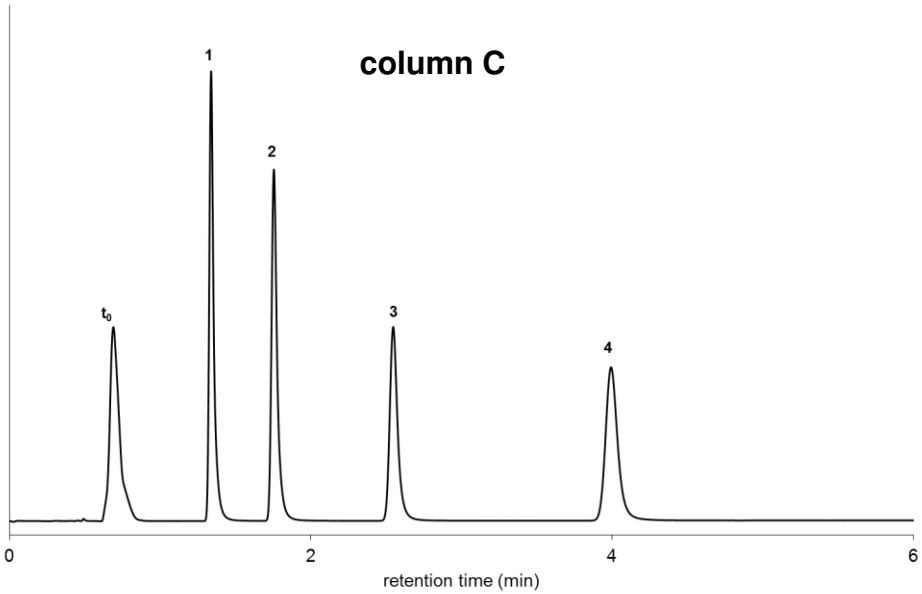
column C
1
2
t0
3
4
0
2
4
6
retention time (min)

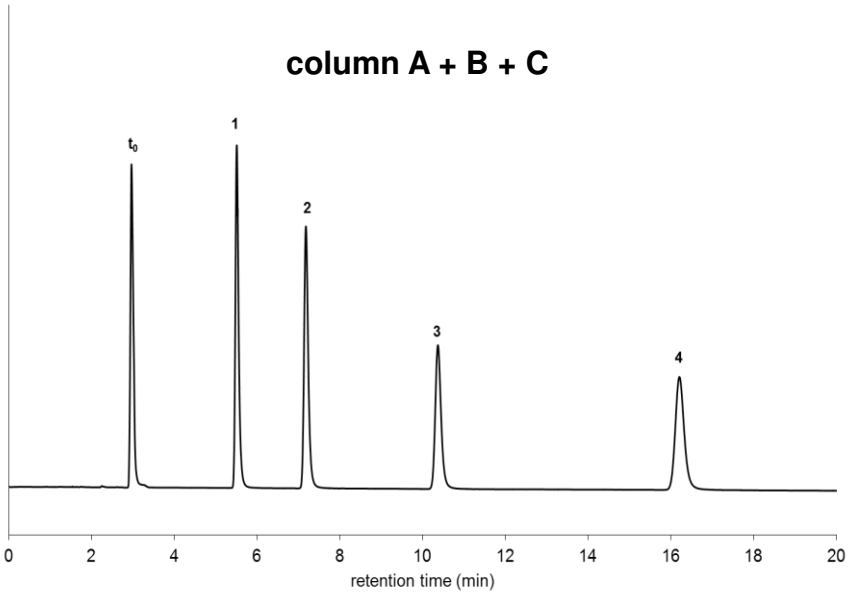
column A + B + C
t0
1
2
3
4
0
2
4
6
8
10
12
14
16
18
20
retention time (min)

Figure 2

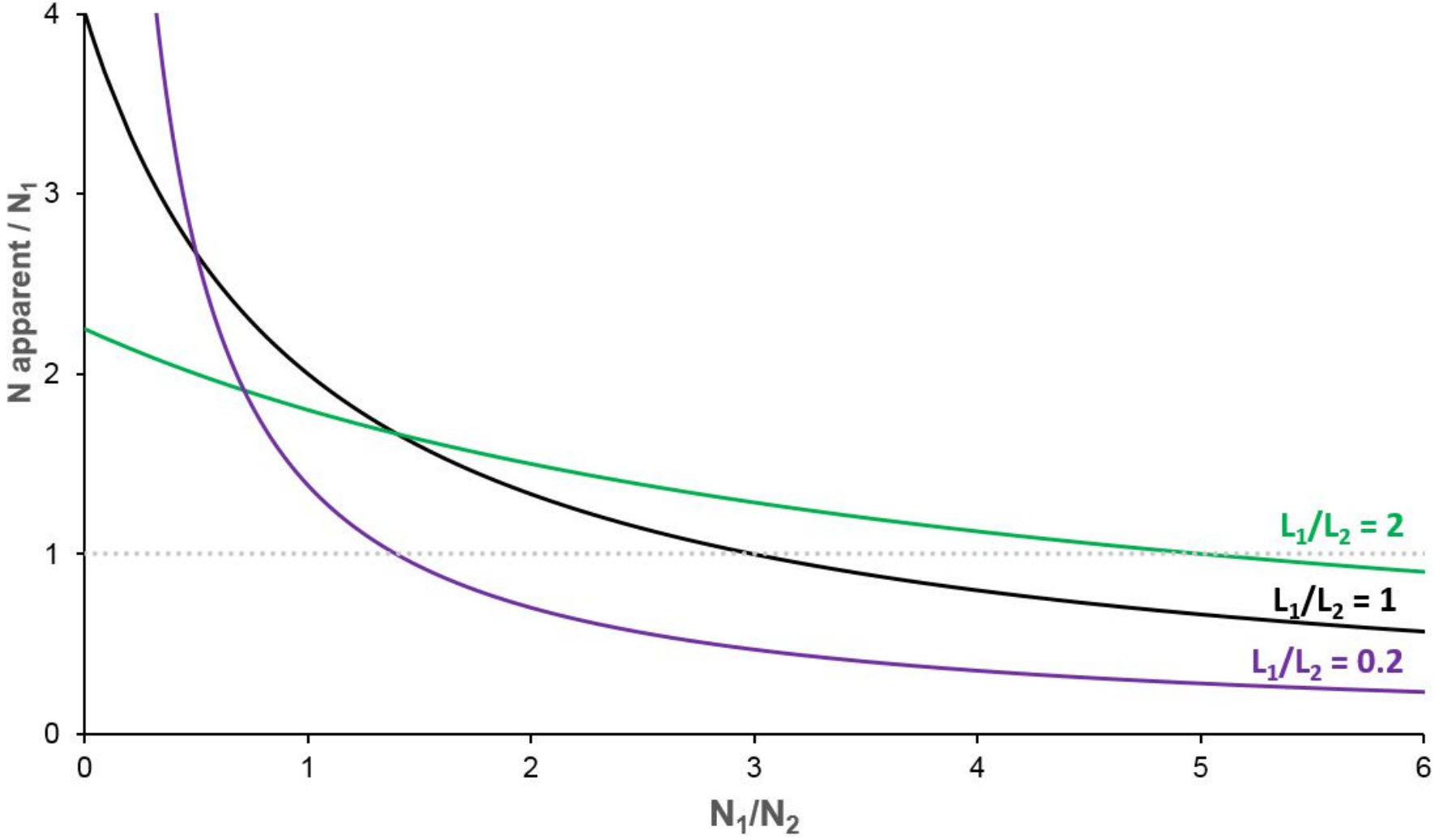

Figure 3

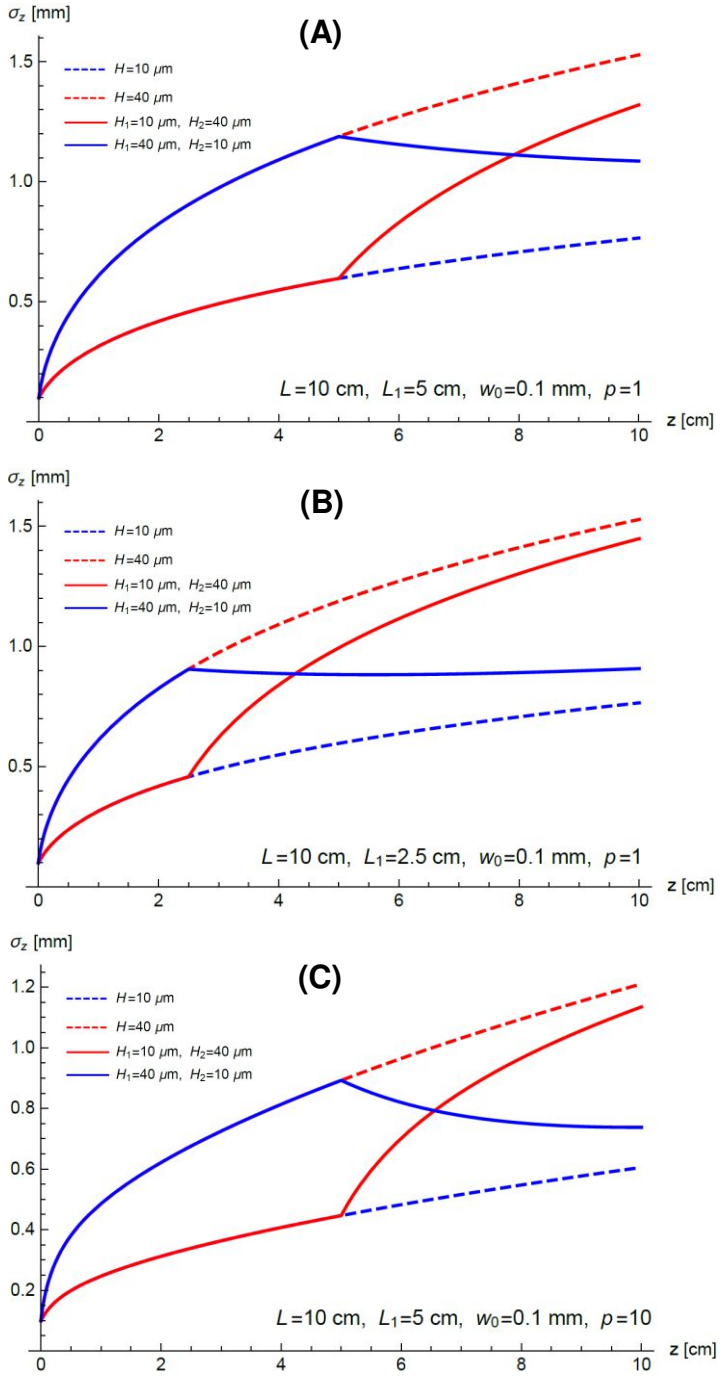
(A)
σz [mm]
H=10 μm
H=40 μm
H1=10 μm, H2=40 μm
H1=40 μm, H2=10 μm
L=10 cm, L1=5 cm, w0=0.1 mm, p=1
z [cm]
(B)
σz [mm]
H=10 μm
H=40 μm
H1=10 μm, H2=40 μm
H1=40 μm, H2=10 μm
L=10 cm, L1=2.5 cm, w0=0.1 mm, p=1
z [cm]
(C)
σz [mm]
H=10 μm
H=40 μm
H1=10 μm, H2=40 μm
H1=40 μm, H2=10 μm
L=10 cm, L1=5 cm, w0=0.1 mm, p=10
z [cm]

Figure 4

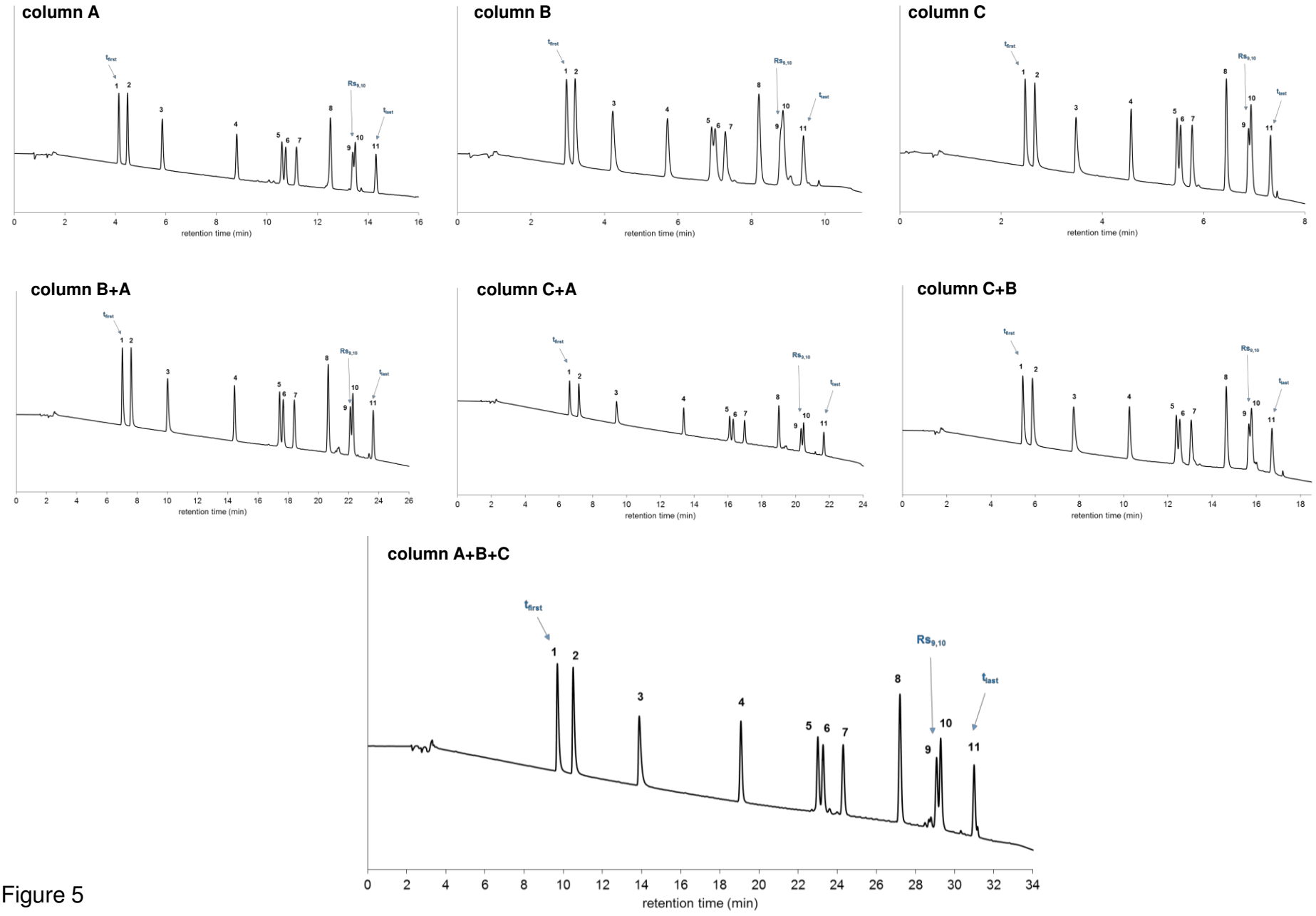
column A
column B
column C
column B+A
column C+A
column C+B
column A+B+C
retention time (min)

Figure 5

column D

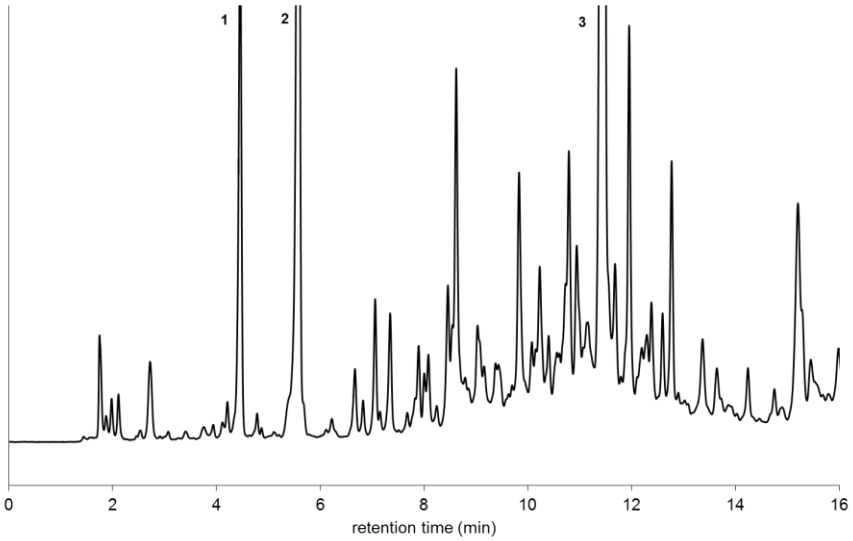

column E

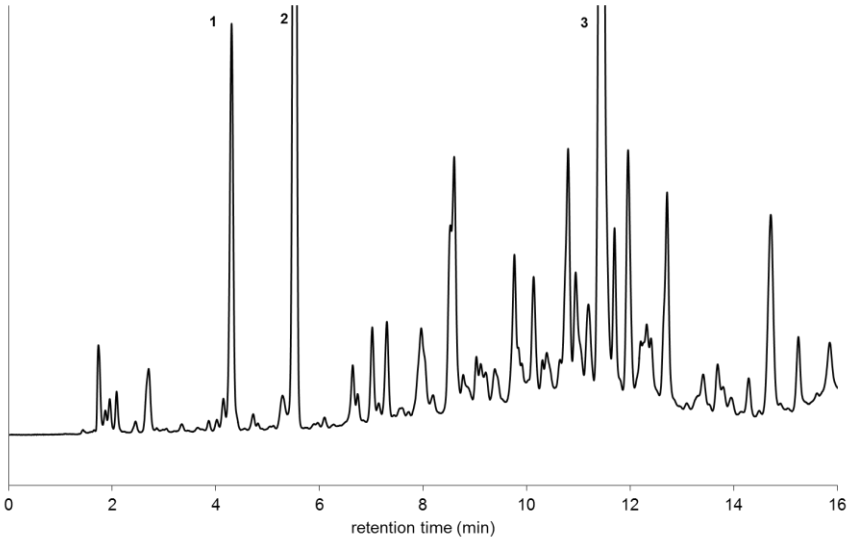

column D + E

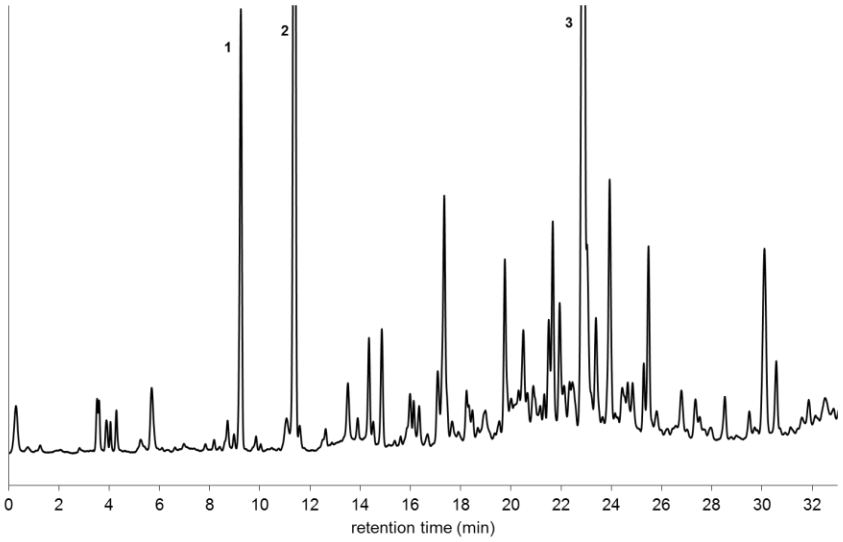

column E + D

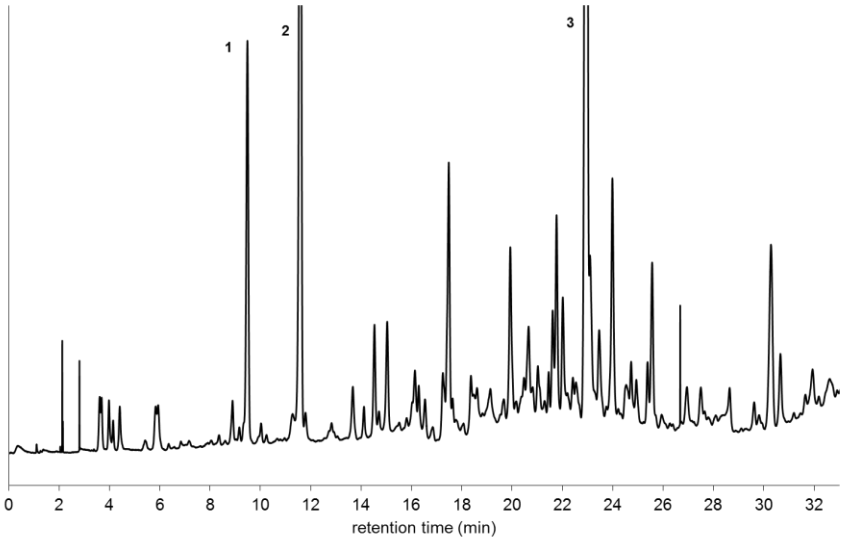

Figure 6